Some theory of a dual-polarization interferometer for sensor applications

R A Abram and S Brand

Department of Physics, Durham University, Durham, DH1 3LE

Abstract.
It is shown that by making straightforward approximations it is possible to simplify the analysis of the measurements of a well-established dual-waveguide interferometer for sensor applications. In particular we derive approximate algebraic formulae for the mode phase shifts that are measured in the interferometric sensor when a layer of the entity to be detected is deposited. Knowledge of the shifts of both the TE and TM mode phases allows the deduction of both the thickness and refractive index of a homogeneous deposited layer, and the formulae derived make that possible with significantly reduced numerical computation. More generally the algebraic formulae and the ease with which numerical results can be obtained for a wide range of layer parameter combinations provide opportunities to improve our understanding of device behaviour. In an application of the theory to a specific practical structure, the numerical results show that the ratio of the TE and TM mode phase shifts varies linearly with deposited layer refractive index but is only weakly dependent on layer thickness, as has been observed previously in some experiments. The numerical results are interpreted using the theory and a simple formula describing the linear dependence of phase shift ratio on deposited layer refractive index is derived.

1. Introduction

Cross and co-workers [1–6] have described in a series of papers the principles and some applications of a sensor based on a particular design of dual-waveguide interferometer. The basic structure is two parallel dielectric slab waveguides each with just one mode of each polarization (TE and TM) sharing a common cladding layer that is sufficiently thick that the two guides operate in an effectively independent manner. The other cladding layer of the upper waveguide is a liquid medium, for example water, in which some entity is to be sensed. In the simplest method of operation, the entity is deposited on the core of the upper waveguide creating an additional homogeneous layer (adlayer) as part of the cladding as shown in figure 1. The deposition results in different changes in the propagation constants of the two modes of the upper waveguide, and hence to phase shifts which can be measured separately by reference to the phases of the corresponding modes of the lower waveguide. This is a particular attraction of the device because a unique combination of deposited layer thickness and index is defined by the measured phase shifts of the two polarizations. Because of this facility, the device is often referred

to and has been marketed as a 'dual-polarization interferometer'. The dual-polarization interferometer is just one type of sensor based on integrated planar optical waveguide interferometry and the reader is referred to the recent review of Kozma *et al* [7] for information on other devices and the relative advantages of the dual-polarization device

The basic theory of planar optical waveguides is very well developed and its application to the theory of sensor performance such as device sensitivity (rate of change of phase with some relevant refractive index and/or a layer thickness in the structure) [8,9] has also received substantial attention. For the specific task of obtaining both the refractive index and thickness of a deposited layer with a dual-polarization interferometer sensor, the approach has been to calculate numerically a continuous set of combinations of deposited layer thickness and refractive index that could lead to the measured TE mode phase shift, using a transfer matrix method for example [4], and then to do the same for the TM mode. It is then possible to obtain the combination of layer thickness and refractive index that is compatible with both the TE and TM mode phase shifts. Further details are given in two theses [10, 11] along with reports of the use of numerical calculations to determine the structural limitations on the precision of the device. While the amount of numerical computation required to deduce the layer thickness and refractive index from the phase shifts is not a major resource issue, it would still be useful to have a straightforward semi-analytical, albeit approximate, method of calculating the mode phase shifts resulting from the deposition of an adlayer to facilitate the interpretation of experimental measurements in general as well as the determination of the parameters of specific adlayers. In this paper we describe just such a method.

In section 2 we briefly review the basic theoretical model used to describe the waveguide modes and show how the analysis can be approximated to obtain explicit expressions for the changes of the propagation constants of the TE and TM modes that result from the introduction of an adlayer into the structure. The efficacy of the theoretical approach is then illustrated in section 3 by considering the effect of adlayers with a range of thickness and refractive index combinations on the modes of a certain structure that has been used for dual-waveguide interferometry.

2. Theory

2.1. Basic model

We consider the modes of the upper planar waveguide of a dual-waveguide interferometer which has the layer structure shown in figure 1. All the layers are assumed to be non-magnetic dielectrics. The core is a solid layer of thickness d and refractive index n_1 and the cladding below it is also a solid with refractive index $n_3 < n_1$. The upper cladding comprises a deposited layer (the adlayer) of thickness a and refractive index n_a, which the interferometer is designed to sense, and a liquid medium, with refractive index $n_2 < n_1$, in which the deposition takes place. In the theory described here the

waveguide is assumed to have infinite width and the lower cladding and the top layer of the upper cladding to have infinite thickness.
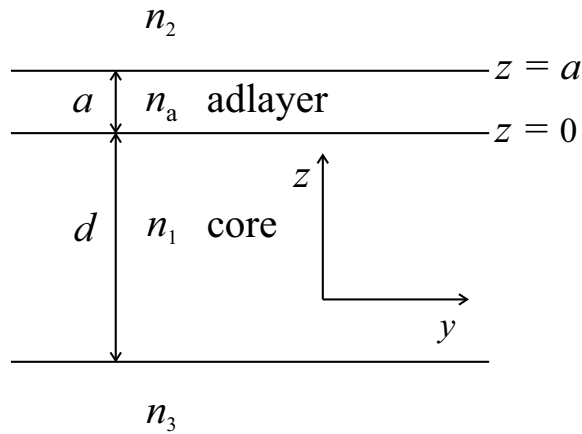
n_2

$z = a$

a | n_a adlayer

$z = 0$

z

d | n_1 core

y

n_3

Figure 1. Schematic diagram of the upper waveguide of the dual-waveguide interferometer. The core has a refractive index n_1 and thickness d. The upper cladding comprises a liquid of refractive index n_2 and also, after its deposition, an adlayer of refractive index n_a and thickness a. The lower cladding, which has refractive index n_3, is also the upper cladding of the lower (reference) waveguide, the rest of which is not shown. The guided modes are confined to the vicinity of the core in the z-direction and are considered to propagate in the y-direction

The waveguide is designed to have one TE and one TM guided mode, each of which can be considered to be plane waves that undergo multiple total internal reflection within the layered structure resulting in net propagation parallel to the layers in the y-direction. The condition for each mode to exist is that the phase change in the wave when it undergoes a round trip in the z-direction, which is transverse to the waveguide plane, is zero or an integer multiple of 2π [12]. It is convenient to consider that phase change to consist of three components, viz, that in traversing the thickness of the core twice and those on the reflections at the core-adlayer and core-lower cladding interfaces. The appearance of an adlayer in the upper cladding causes changes in the propagation constants of the modes of the waveguide and hence shifts in the phase changes of the modes that occur when they propagate along the waveguide. In the dual-waveguide interferometer those phase shifts can be measured by reference to the phases of the corresponding modes of the lower waveguide of the device (which is not shown in the figure).

2.2. TE modes

The TE modes have an electric field component E_x and magnetic field components B_y and B_z. They can be considered to result from the multiple total reflections of a plane wave propagating in the y-z plane in the core with electric field parallel to the x-axis. A mode with propagation constant k_y corresponds to a plane wave which in the core propagates at an angle θ to the waveguide plane where $\cos\theta = k_y/n_1 k_0$. We can cal-

culate the reflection coefficient of such a wave at the core-adlayer interface (taken to be located at $z = 0$) by using a transfer matrix method. The incident and reflected field components parallel to the plane of the interface can be written as

Incident:

$$E_x = E_0 \exp(ik_y y + ik_z z) \tag{1}$$
$$cB_y = (k_z/k_0)E_0 \exp(ik_y y + ik_z z) \tag{2}$$

Reflected:

$$E_x = r_{te}E_0 \exp(ik_y y - ik_z z) \tag{3}$$
$$cB_y = -r_{te}(k_z/k_0)E_0 \exp(ik_y y - ik_z z) \tag{4}$$

where a time dependence $\exp(-i\omega t)$ has been assumed but is not shown explicitly, E_0 is a constant defining the amplitude of the incident electric field, c is the velocity of light in free space, $k_0 = \omega/c$, r_{te} is the reflection coefficient to be determined of a TE polarized wave incident from the core on the upper cladding, and

$$k_z = (n_1^2 k_0^2 - k_y^2)^{\frac{1}{2}}. \tag{5}$$

The field components of the waves in all the layers of the structure must have the same y-dependence as the fields in equations 1-4. Also for a bound mode it is necessary for the wave in the core to be totally reflected by the upper and lower cladding. Total reflection by the upper cladding requires that $k_y = n_1 k_0 \cos\theta > n_2 k_0$ and then the relevant field components in the top layer of the upper cladding have the form

$$E_x = t_{te}E_0 \exp(ik_y y - \alpha(z - a)) \tag{6}$$
$$cB_y = it_{te}(\alpha/k_0)E_0 \exp(ik_y y - \alpha(z - a)), \tag{7}$$

where t_{te} is a constant defining the amplitude of the electric field at $z = a$ and

$$\alpha = (k_y^2 - n_2^2 k_0^2)^{\frac{1}{2}}. \tag{8}$$

The values of E_x and cB_y in the adlayer at $z = a$ can be related to those at $z = 0$ by the transfer matrix across the adlayer for the fields, which in the basis (E_x, cB_y) is

$$M_{te}(a) = \begin{pmatrix} \cosh\gamma a & i(k_0/\gamma)\sinh\gamma a \\ -i(\gamma/k_0)\sinh\gamma a & \cosh\gamma a \end{pmatrix} \tag{9}$$

where, without loss of generality, $M(a)$ has been written in the form appropriate to the case $k_y > n_a k_0$ so that

$$\gamma = (k_y^2 - n_a^2 k_0^2)^{\frac{1}{2}} \tag{10}$$

is a real positive quantity. Also, since the fields E_x and cB_y are continuous at the layer interfaces, we can use the same transfer matrix to relate the fields in the top layer of the cladding at $z = a$ to the fields in the core at $z = 0$:

$$M_{te}(a) \begin{pmatrix} 1 + r_{te} \\ (k_z/k_0)(1 - r_{te}) \end{pmatrix} = \begin{pmatrix} t_{te} \\ it_{te}(\alpha/k_0) \end{pmatrix}. \tag{11}$$

Using the two equations represented by the matrix equation 11 to eliminate t_{te}, we can obtain an expression for the reflection coefficient of the cladding determined at $z = 0$:

$$r_{te} = \frac{F_{te} + G_{te}}{F_{te}^* + G_{te}^*} \tag{12}$$

where

$$F_{te} = -(k_z/k_0)[\cosh \gamma a + (\alpha/\gamma) \sinh \gamma a]$$

and

$$G_{te} = i(\alpha/k_0)[\cosh \gamma a + (\gamma/\alpha) \sinh \gamma a].$$

It is apparent from the structure of the right hand side of equation 12 that the magnitude of r_{te} is unity. The phase is given by

$$\delta_{te}^{uc}(k_y) = -2 \arctan \left[\left(\frac{\gamma}{k_z} \right) \left(\frac{\alpha \cosh \gamma a + \gamma \sinh \gamma a}{\gamma \cosh \gamma a + \alpha \sinh \gamma a} \right) \right]. \tag{13}$$

When there is no adlayer, $a = 0$ and then the phase of the reflection coefficient is

$$\delta_{te}^{uc0}(k_y) = -2 \arctan \left(\frac{\alpha}{k_z} \right). \tag{14}$$

This result can also be used to obtain the reflection coefficient and phase change on reflection at the core-lower cladding interface. The lower cladding never contains an adlayer but the refractive index n_3 is generally different from that of the upper cladding (n_2). Nevertheless, that refractive index must be such that the condition $k_y > n_3 k_0$ holds so that total reflection occurs and a guided mode results. This being the case, the reflection coefficient determined at $z = -d$ has unit magnitude and a phase

$$\delta_{te}^{lc}(k_y) = -2 \arctan \left(\frac{\beta}{k_z} \right), \tag{15}$$

where

$$\beta = (k_y^2 - n_3^2 k_0^2)^{\frac{1}{2}}. \tag{16}$$

The third component in the phase change in a transverse round trip of a doubly reflected plane wave is due to the transit across the thickness d of the core and back, which gives

$$\delta_{te}^{tr}(k_y) = 2k_z d. \tag{17}$$

The structure of the interferometer is designed so that in the absence of an adlayer it can support just one TE mode at the operating frequency ω. The value of the propagation constant k_y of that mode, which we denote by κ_0, can be obtained by solving the equation

$$\delta_{te}^{uc0}(\kappa_0) + \delta_{te}^{lc}(\kappa_0) + \delta_{te}^{tr}(\kappa_0) = 2\pi m \tag{18}$$

where m is zero or an integer. Equation 18 is well known in waveguide theory and its solution reduces to a numerical root-finding exercise. When an adlayer has been deposited in the waveguide structure, the propagation constant of the mode changes to

a different value, which we denote by κ and the essential feature of the interferometer is that it gives the change in propagation constant $\Delta\kappa = \kappa - \kappa_0$ through a phase shift measurement. A theoretical value for the change in propagation constant can be obtained by carrying out a numerical solution of

$$\delta_{te}^{uc}(\kappa) + \delta_{te}^{lc}(\kappa) + \delta_{te}^{tr}(\kappa) = 2\pi m. \tag{19}$$

for κ.

While a full numerical calculation of $\Delta\kappa$ is straightforward and quantitatively reliable, further analysis can provide additional insight into the behaviour of the interferometer as well as facilitating a simpler, albeit approximate, numerical solution that could be helpful in interpreting measurements. If κ_0 has already been calculated, we can take the difference of equations 19 and 18 and use the component approximations

$$\delta_{te}^{j}(\kappa) = \delta_{te}^{j}(\kappa_0) + \left.\frac{d\delta_{te}^{j}}{d\kappa}\right|_{\kappa=\kappa_0} \Delta\kappa$$

for $j = uc, lc, tr$ to write

$$\Delta\kappa = \frac{\delta_{te}^{uc0}(\kappa_0) - \delta_{te}^{uc}(\kappa_0)}{\left[d\delta_{te}^{uc}/d\kappa + d\delta_{te}^{lc}/d\kappa + d\delta_{te}^{tr}/d\kappa\right]_{\kappa=\kappa_0}}. \tag{20}$$

In deriving equation 20 we have tacitly assumed that while the change of phase $\delta_{te}^{uc}(\kappa_0) - \delta_{te}^{uc0}(\kappa_0)$ of the reflection coefficient r_{te} when an adlayer is introduced can be substantial, and is not readily expressed in an approximate algebraic form, the change of phase with the propagation constant κ is generally well represented by the linear term in a Taylor series.

The individual terms in equation 20 can be resolved as follows. Making use of equations 5, 8, 10 and 16 with the propagation constant $k_y = \kappa$, we can obtain

$$\frac{d\delta_{te}^{tr}}{d\kappa} = -\frac{2\kappa d}{k_z} \tag{21}$$

from equation 17,

$$\frac{d\delta_{te}^{lc}}{d\kappa} = -\frac{2\kappa}{\beta k_z} \tag{22}$$

from equation 15, and from equation 13,

$$\frac{d\delta_{te}^{uc}}{d\kappa} = -2\kappa k_0^2 \left(\frac{A_{te}}{1 + A_{te}^2}\right) \left[\frac{(n_1^2 - n_a^2)}{\gamma^2 k_z^2} + \frac{(k_z/\alpha)(1 + \alpha a)(n_2^2 - n_a^2)}{N_{te}D_{te}}\right], \tag{23}$$

where

$$N_{te} = \gamma \left(\alpha \cosh \gamma a + \gamma \sinh \gamma a\right) \tag{24}$$

$$D_{te} = k_z \left(\gamma \cosh \gamma a + \alpha \sinh \gamma a\right) \tag{25}$$

$$A_{te} = N_{te}/D_{te}. \tag{26}$$

If the adlayer is very thin so that $\gamma a \ll 1$, we can write

$$\delta_{te}^{uc0}(\kappa_0) - \delta_{te}^{uc}(\kappa_0) = -a \left.\frac{d\delta_{te}^{uc}(\kappa)}{da}\right|_{\substack{a=0 \\ \kappa=\kappa_0}} = -2k_z a \left(\frac{n_a^2 - n_2^2}{n_1^2 - n_2^2}\right) \tag{27}$$

(with k_z evaluated for $k_y = \kappa_0$) and use that result in equation 20 along with

$$\frac{d\delta_{te}^{uc}}{d\kappa} \approx \left.\frac{d\delta_{te}^{uc}}{d\kappa}\right|_{a=0} = -\frac{2\kappa}{\alpha k_z} \tag{28}$$

and equations 21 and 22 to obtain the leading term in $\Delta\kappa$, which is proportional to a. It is convenient to write the result in terms of the effective refractive index of the mode $n_{te} = \kappa/k_0$ and specifically the change $\Delta n_{te} = \Delta\kappa/k_0$ from its value $n_{te0} = \kappa_0/k_0$ in the absence of an adlayer:

$$\Delta n_{te} = \frac{a}{d_{te}}\left[\frac{(n_1^2 - n_{te0}^2)(n_a^2 - n_2^2)}{n_{te0}(n_1^2 - n_2^2)}\right], \tag{29}$$

where $d_{te} = d + \alpha^{-1} + \beta^{-1}$ (with α and β evaluated for $k_y = \kappa_0$) is an effective extent in z of the TE mode fields.

The corresponding sensitivity of the sensor to the appearance of an adlayer $(\partial n_{te}/\partial a|_{a=0})$ is trivial to calculate from equation 29 and is identical to the result for $a = 0$ obtained by Tiefenthaler and Lukosz [8], which has recently been extended to $a \neq 0$ by Sharma *et al* [9].

2.3. TM modes

For the TM modes, the plane wave equations corresponding to equations 1-4 and 6-7 are

Incident:

$$\begin{aligned} E_y &= E_0 \exp(ik_y y + ik_z z) \\ cB_x &= (-n_1^2 k_0/k_z)E_0 \exp(ik_y y + ik_z z) \end{aligned}$$

Reflected:

$$\begin{aligned} E_y &= r_{tm}E_0 \exp(ik_y y - ik_z z) \\ cB_x &= r_{tm}E_0(n_1^2 k_0/k_z)\exp(ik_y y - ik_z z) \end{aligned}$$

Top layer of upper cladding:

$$\begin{aligned} E_y &= t_{tm}E_0 \exp(ik_y y - \alpha(z-a)) \\ cB_y &= it_{tm}(n_2^2 k_0/\alpha)E_0 \exp(ik_y y - \alpha(z-a)), \end{aligned}$$

The transfer matrix across the adlayer is

$$M_{tm}(a) = \begin{pmatrix} \cosh\gamma a & i(\gamma/n_a^2 k_0)\sinh\gamma a \\ -i(n_a^2 k_0/\gamma)\sinh\gamma a & \cosh\gamma a \end{pmatrix}$$

and using that we can relate the values of E_y and cB_x at $z = a$ to those at $z = 0$:

$$M_{tm}(a)\begin{pmatrix} 1 + r_{tm} \\ -(n_1^2 k_0/k_z)(1 - r_{tm}) \end{pmatrix} = \begin{pmatrix} t_{tm} \\ it_{tm}(n_2^2 k_0/\alpha) \end{pmatrix}.$$

It follows that the reflection coefficient of the upper cladding determined at $z = 0$ is

$$r_{tm} = \frac{F_{tm} + G_{tm}}{F_{tm}^* + G_{tm}^*},$$

where

$$F_{tm} = -(n_1^2 k_0/k_z)[\cosh \gamma a + (n_2^2 \gamma/n_a^2 \alpha) \sinh \gamma a]$$

and

$$G_{tm} = i(n_2^2 k_0/\alpha)[\cosh \gamma a + (n_a^2 \alpha/n_2^2 \gamma) \sinh \gamma a].$$

The magnitude of r_{tm} is unity and the phase is

$$\delta_{tm}^{uc}(k_y) = \pi - 2 \arctan \left[\left(\frac{\gamma/n_a^2}{k_z/n_1^2} \right) \left(\frac{(\alpha/n_2^2) \cosh \gamma a + (\gamma/n_a^2) \sinh \gamma a}{(\gamma/n_a^2) \cosh \gamma a + (\alpha/n_2^2) \sinh \gamma a} \right) \right].$$

In the absence of an adlayer, $a = 0$, the phase change of the wave on reflection at the upper cladding reduces to

$$\delta_{tm}^{uc0}(k_y) = \pi - 2 \arctan \left(\frac{\alpha/n_2^2}{k_z/n_1^2} \right).$$

The phase change on reflection at the lower cladding is

$$\delta_{tm}^{lc}(k_y) = \pi - 2 \arctan \left(\frac{\beta/n_3^2}{k_z/n_1^2} \right),$$

and the phase change due to the double transit across the core is given by equation 17, as in the TE case.

The TM mode of the structure with and without the adlayer can be found numerically by the procedure described for the TE polarization. The value of the propagation constant k_y (and hence k_z, α, β and γ) will of course be different from the TE case but we use the same symbols (κ_0 and κ) to simplify the notation without any risk of ambiguity. We can also use the TM version of equation 20,

$$\Delta\kappa = \frac{\delta_{tm}^{uc0}(\kappa_0) - \delta_{tm}^{uc}(\kappa_0)}{\left[d\delta_{tm}^{uc}/d\kappa + d\delta_{tm}^{lc}/d\kappa + d\delta_{tm}^{tr}/d\kappa \right]_{\kappa=\kappa_0}}, \tag{30}$$

to obtain a relatively simple approximate formula for $\Delta\kappa$. Again, we must resolve the individual components in equation 30. First we have that

$$\frac{d\delta_{tm}^{tr}}{d\kappa} = -\frac{2\kappa d}{k_z},$$

as for the TE case, and

$$\frac{d\delta_{tm}^{lc}}{d\kappa} = -\frac{2\kappa}{\beta k_z} \left[\left(\frac{n_{tm}}{n_1} \right)^2 + \left(\frac{n_{tm}}{n_3} \right)^2 - 1 \right]^{-1},$$

where $n_{tm} = \kappa/k_0$ is the effective refractive index of the TM mode. Finally

$$\frac{d\delta_{tm}^{uc}}{d\kappa} = -2\kappa k_0^2 \left(\frac{A_{tm}}{1 + A_{tm}^2} \right) \left\{ \frac{(n_1^2 - n_a^2)}{\gamma^2 k_z^2} \right.$$
$$\left. + \left(\frac{k_z/\alpha}{n_a^2 n_1^2 N_{tm} D_{tm}} \right) \left(\frac{n_2^2 - n_a^2}{n_a^2 n_2^2} \right) \left[1 + \alpha a \left(\left(\frac{n_{tm}}{n_a} \right)^2 + \left(\frac{n_{tm}}{n_2} \right)^2 - 1 \right) \right] \right\},$$

where

$$N_{tm} = (\gamma/n_a^2) \left[(\alpha/n_2^2) \cosh \gamma a + (\gamma/n_a^2) \sinh \gamma a \right]$$

$$D_{tm} = (k_z/n_1^2) \left[(\gamma/n_a^2) \cosh \gamma a + (\alpha/n_2^2) \sinh \gamma a \right]$$

$$A_{tm} = N_{tm}/D_{tm}.$$

For a very thin adlayer ($\gamma a \ll 1$),

$$\delta_{tm}^{uc0}(\kappa_0) - \delta_{tm}^{uc}(\kappa_0) \approx - a \left. \frac{d\delta_{tm}^{uc}(\kappa)}{da} \right|_{\substack{a=0 \\ \kappa=\kappa_0}}$$

$$= - 2k_z a \left(\frac{n_a^2 - n_2^2}{n_1^2 - n_2^2} \right) \left(\frac{(n_{tm0}/n_a)^2 + (n_{tm0}/n_2)^2 - 1}{(n_{tm0}/n_1)^2 + (n_{tm0}/n_2)^2 - 1} \right),$$

where n_{tm0} is the effective refractive index in the absence of an adlayer. We can use this together with

$$\frac{d\delta_{tm}^{uc}}{d\kappa} \approx \left. \frac{d\delta_{tm}^{uc}}{d\kappa} \right|_{a=0} = -\frac{2\kappa}{\alpha k_z} \left[\left(\frac{n_{tm}}{n_1} \right)^2 + \left(\frac{n_{tm}}{n_2} \right)^2 - 1 \right]^{-1}$$

in equation 30 along with the formulae for $d\delta_{tm}^{tr}/d\kappa$ and $d\delta_{tm}^{lc}/d\kappa$ to obtain the leading term in the change of effective refractive index Δn_{tm}, which, as with the TE case, is proportional to a. The result is

$$\Delta n_{tm} = \frac{a}{d_{tm}} \left[\frac{(n_1^2 - n_{tm0}^2)(n_a^2 - n_2^2)}{n_{tm0}(n_1^2 - n_2^2)} \right] \left[\frac{(n_{tm0}/n_a)^2 + (n_{tm0}/n_2)^2 - 1}{(n_{tm0}/n_1)^2 + (n_{tm0}/n_2)^2 - 1} \right], \quad (31)$$

where

$$d_{tm} = d + \left\{ \alpha \left[\left(\frac{n_{tm0}}{n_1} \right)^2 + \left(\frac{n_{tm0}}{n_2} \right)^2 - 1 \right] \right\}^{-1} + \left\{ \beta \left[\left(\frac{n_{tm0}}{n_1} \right)^2 + \left(\frac{n_{tm0}}{n_3} \right)^2 - 1 \right] \right\}^{-1}$$

is an effective extent in z of the TM mode fields. The corresponding sensor sensitivity ($\partial n_{tm}/\partial a|_{a=0}$) is the same as the result for $a = 0$ previously obtained by Tiefenthaler and Lukosz [8].

3. An illustrative example

As an illustrative example of the application of the theory in section 2 we consider the effect of an adlayer on the modes of a waveguide with the parameter values given in table 1, which are those of a structure used in the work reported in [6]. In the absence of an adlayer the waveguide considered has modes with effective refractive indexes (to six significant figures), $n_{te0} = 1.50754$ and $n_{tm0} = 1.50648$ when excited by a helium-neon laser with a free space wavelength of 632.8 nm. To demonstrate the effectiveness of the approximate method for calculating how the effective refractive index of a mode((which henceforth we refer to as the 'mode index' for brevity) is affected by an adlayer, we compare the results obtained using equations 20 (TE mode) and 30 (TM mode) with those from a full numerical solution of equations 18 and 19 (TE mode), and the corresponding equations for the TM case.

n_1	n_2	n_3	d (nm)
1.524	1.331	1.475	998

Table 1. Values of the waveguide parameters defined in figure 1 that have been used to obtain the results presented in section 3.
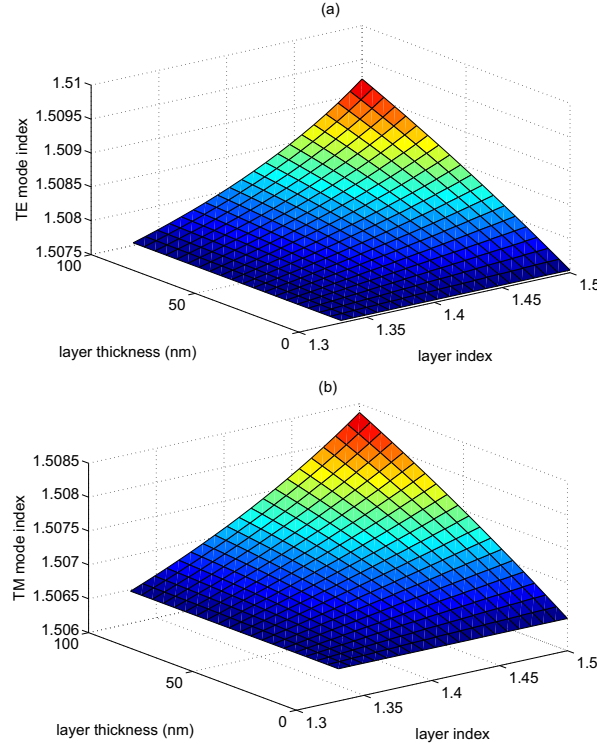

Figure 2. The calculated mode index as a function of adlayer thickness and refractive index for (a) the TE mode and (b) the TM mode of the structure shown in figure 1 with the parameters given in table 1.

Figure 2 shows the results obtained using equations 20 (TE mode) and 30 (TM mode) for the dependence of the TE and TM mode indexes on adlayer thickness ($0 \leq a \leq 100$nm) and refractive index ($1.331 \leq n_a \leq 1.5$), where the lower limit of the refractive index is the value for the water cladding layer in the absence of an adlayer. The percentage error in the calculated mode index relative to the value obtained from a full numerical calculation is greatest for the most extreme case considered ($a = 100$nm, $n_a = 1.5$) where it is only 0.003%, and it is substantially less than that over most of the range of parameters considered. However, it is the *change* of mode index that is measured by the interferometer and being much smaller than the value of the mode index itself, the percentage error is significantly larger. The results in figure 3 suffer from numerical noise near $a = 0$ and $n_a = n_2 = 1.331$ and show errors approaching 3% at the largest a and n_a considered.

Experimental measurements of the TE and TM mode index changes for a structure with a specific adlayer define contours on the surfaces of figure 3, which correspond to
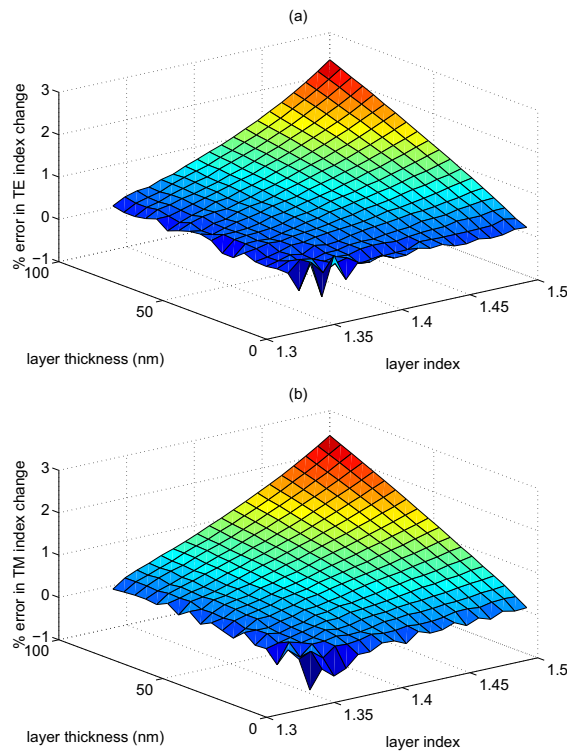
Figure 3. The percentage error in the calculated change of (a) the TE mode index and (b) the TM mode index shown in figure 2 relative to the change obtained using a full numerical method.

the possible combinations of layer thickness and refractive index that could give rise to the mode index change for each polarization. The intersection of those contours in the layer thickness-refractive index plane determines, to within experimental and theoretical error, the unique combination that is compatible with the results for both polarizations.
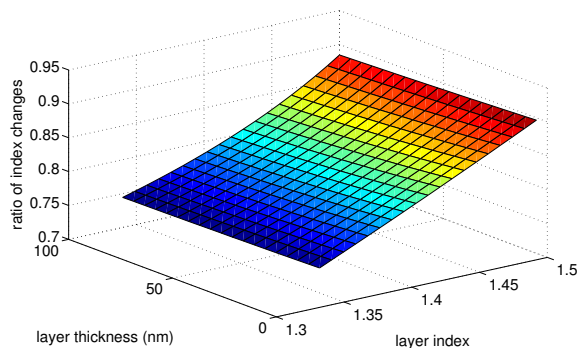

Figure 4. Ratio of the calculated TE to TM mode index changes versus adlayer thickness and refractive index.

Figure 4 shows how the ratio of the TE to TM mode index changes with adlayer thickness and refractive index. The ratio shows a near-linear increase with increasing layer index. However, the ratio is strikingly insensitive to layer thickness, a property

previously observed and remarked on by Cross [6] for a similar structure. The theory provides a simple qualitative explanation for the weak dependence of the TE-TM index ratio on layer thickness and also the formulae for a quantitative description. We have shown that for both polarizations the leading term in the expression for the change in mode index for small a ($\gamma a \ll 1$) is proportional to a and also we know from simple physical considerations that the change in mode index will be independent of a for sufficiently thick layers. It follows that the ratio of mode index changes is insensitive to change in a for both small and large a. In the case of small a we can use the formulae derived at the ends of sections 2.2 and 2.3 to predict the dependence of the ratio on change of adlayer refractive index n_a.

Using equations 29 and 31, we can write the ratio

$$\frac{\Delta n_{te0}}{\Delta n_{tm0}} = \left[\frac{n_{tm0}d_{tm}}{n_{te0}d_{te}}\right] \left[\frac{(n_1^2 - n_{te0}^2)}{(n_1^2 - n_{tm0}^2)}\right] \left[\frac{(n_{tm0}/n_1)^2 + (n_{tm0}/n_2)^2 - 1}{(n_{tm0}/n_a)^2 + (n_{tm0}/n_2)^2 - 1}\right]. \quad (32)$$

The denominator of the third factor on the right hand side of equation 32 is the only term dependent on n_a. Recognizing that $(n_a - n_2)/n_2 \ll 1$ for $n_2 = 1.331$ and the range of values of n_a displayed in figure 4, the term may be written as

$$\left[\left(\frac{n_{tm0}}{n_a - n_2 + n_2}\right)^2 + \left(\frac{n_{tm0}}{n_2}\right)^2 - 1\right]^{-1}$$

and expanded up to first order in $(n_a - n_2)/n_2$ to give

$$\frac{1}{[2(n_{tm0}/n_2)^2 - 1]} \left\{1 + \frac{2(n_{tm0}/n_2)^2}{2(n_{tm0}/n_2)^2 - 1}\left(\frac{n_a - n_2}{n_2}\right) + \cdots \right\}. \quad (33)$$

For the relevant range of n_a, equation 33 provides an excellent approximation to the original expression and its use in equation 32 with the parameters in table 1 gives excellent quantitative agreement with the linear dependence of $\Delta n_{te0}/\Delta n_{tm0}$ on n_a as $a \to 0$ that is seen in figure 4.

4. Conclusions

We have given a concise description of the theory of a dual-polarization interferometer for sensor applications and have proceeded to show how some simple approximations facilitate the derivation of formulae for the mode phase shifts that are observed in the interferometer with the deposition of a layer of the entity to be detected. It has already been explained by other authors that knowledge of the phase shifts of both the TE and TM modes allows the deduction of both the thickness and refractive index of a homogeneous deposited layer, but the formulae derived here make that possible with much less numerical computation than has been required hitherto. Also, the numerical results obtained for a specific device support the contention that the ratio of the TE and TM phase shifts increases linearly with increasing layer refractive index but is only weakly dependent on layer thickness. Furthermore the theory developed provides both a qualitative explanation and a quantitative description of that behaviour.

Acknowledgments

References

[1] Graham H Cross, Yitao Ren, and Neville J Freeman. Young's fringes from vertically integrated slab waveguides: Applications to humidity sensing. *J. Appl. Phys.*, 86:6483–88, 1999.

[2] Graham H Cross, Andrew A Reeves, Stuart Brand, Jonathan F Popplewell, Louise L Peel, Marcus J Swann, and Neville J Freeman. A new quantitative optical biosensor for protein characterisation. *Biosensors and Bioelectronics*, 19:383–90, 2003.

[3] Neville J Freeman, Louise L Peel, Marcus J Swann, Graham H Cross, Andrew Reeves, Stuart Brand, and Jian R Lu. Real time, high resolution studies of protein adsorption and structure at the solid-liquid interface using dual polarization interferometry. *J. Phys.: Condens. Matter*, 16:S2493–6, 2004.

[4] Graham H Cross, Andrew Reeves, Stuart Brand, Marcus J Swann, Louise L Peel, Neville J Freeman, and Jian R Lu. The metrics of surface adsorbed small molecules on the Young's fringe dual slab waveguide interferometer. *J. Phys. D: Appl. Phys.*, 37:74–80, 2004.

[5] Osbert Tan and Graham H Cross. Surface anchoring structure of a liquid crystal monolayer studied via dual polarization interferometry. *Phys. Rev. E*, 79:021703, 2009.

[6] Graham Hugh Cross. Fundamental limit to the use of effective medium theories in optics. *Optics Letters*, 38:3057–60, 2013.

[7] Peter Kozma, Florian Kehl, Eva Ehrentreich-Förster, and Christoph Stamm. Integrated planar optical waveguide interferometer biosensors: a comparitive review. *Biosensors and Bioelectronics*, 58:287, 2014.

[8] K. Tiefenthaler and W Lukosz. Sensitivity of grating couplers as integrated-optical chemical sensors. *J. Opt. Soc. Am. B*, 6:209, 1989.

[9] Gaurav Sharma, Sushil Kumar, and Vivek Singh. Rigorous analysis of the sensitivity of three layer planar optical waveguides having an adlayer. *Opt. Comm.*, 315:333, 2014.

[10] A A Reeves. *Theoretical studies of one-dimensional and two-dimensional photonic structures.* Durham University Thesis, 2004.

[11] Zheng Tan. *Optical studies of ordered monomolecular layers: Ab-initio simulation and experiment.* Durham University e-Thesis, 2009.

[12] J D Jackson. *Classical Electrodynamics.* Wiley, 3rd edition, 1999.